PERIODICA POLYTECHNICA SER. TRANSP. ENG. VOL. 34, NO. 1–2, PP. 69–84 (2006)

STATISTICAL EVALUATION OF NUMBER AND DIMENSION OF DEFECTS IN STEEL BEFORE AND AFTER FATIGUE TEST BASED ON X-RAY EXAMINATION[1]

István ZOBORY*, Tamás UNGÁR**, Anatoly SNIGIREV***, József GYŐRI* and Elemér BÉKEFI*

*Department of Railway Vehicles
Faculty of Transportation Engineering
Budapest University of Technology and Economics
H–1521 Budapest, Hungary
**Department of General Physics
Faculty of Science Eötvös University Budapest
P.O.Box. 32, H–1518 Budapest Hungary
***ESRF
6 rue Jules Horowitz
BP 220
F–38043 Grenoble Cedex 9
France

Received: November 10, 2004

Abstract

Several scientific research purpose and practical engineering problems make it necessary to get information on the number and statistical characteristics of micro and meso defects existing in steel materials both in 'virgin' state and after loads exerted in the course of high cycle fatigue tests. In this paper the measurement results received from of X-ray measurements carried out in Grenoble (France) using the *sinkrotron* equipment at the the ESRF Beamline ID22 Laboratory in order to get quantitative information about distribution and dimension of defects in steel material specimens are introduced.

Keywords: defects in steel, distribution of defects, X-ray measurements, statistical evaluation.

1. Introduction

Dimensioning for reliability is a central problem in the modern engineering design. There are several known methods for analysing complicated large-scale mechanical systems if the reliability functions or the failure rate functions of the components are known. Unfortunately in general this is not the case, since data on the service life distribution or failure rate only for the most severally loaded components are available on the basis of fatigue tests. It is a challenge for the researchers to try to

[1]This research was supported by the National Scientific Research Fund (OTKA). Grant No T038399

determine the reliability functions of machine components by means of computer simulation based on the geometrical data of the volume occupied by the component and the density, orientation and dimensions of the micro cracks distributed within the volume mentioned. In order to get information about the latter data a joint research activity was launched by the Department of Railway Vehicles at the Budapest University of Technology and Economics (BME) and the Department of General Physics at the Eötvös University Budapest (ELTE) to carry out X-ray examinations on thin slice specimens processed of structural steel material. In order to prepare the experimental activity, small disc form thin slice specimens of diameter of 6 mm and thickness of 0.1 mm were processed from a steel specimen material before and after fatigue test continued up to fracture. The X-ray examinations were carried out in *Grenoble* (France), using the equipment of the ESRF Beamline ID22 Laboratory in the framework of an international scientific co-operation project.

2. The Steel Material Examined

The material examined was a structural steel frequently used in vehicle components. In *Fig. 1* taken by energy dispersion X-ray analysis (EDS analysis) the content of the basic material (ferrum) and the alloying elements are shown.

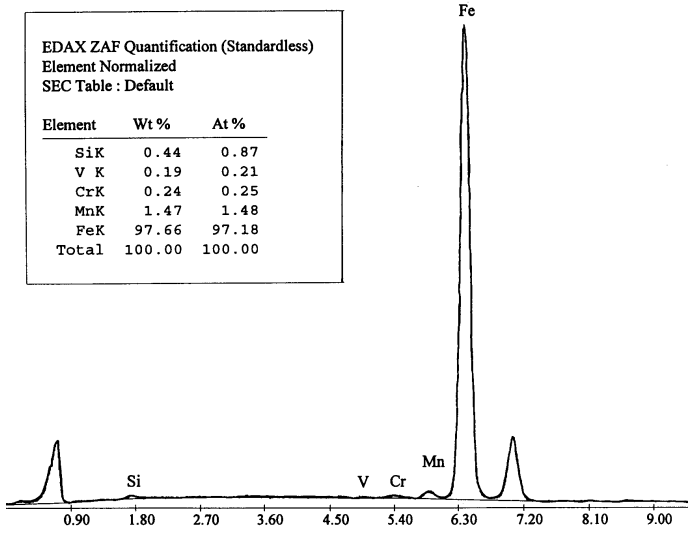

Fig. 1. Energy dispersion X-ray analysis map of the steel examined

On the horizontal axis the energy level is indicated in kiloelectronvolt, while on the vertical axis quantities proportional to the mass percent of the components being present are indicated. As it can be observed, the material examined can practically be considered as alloying-free steel, since it has only slight manganese

content, less then 1.5%, and practically negligible chromium, vanadium and silicon contents.

3. Preparation of Specimens for X-Ray Examination

The specimens prepared for the X-ray examination were thin circular disc-form ones of 0.1 mm width processed from fatigue test specimen by extra fine laboratory purpose sawing machine operating under low cutting speed conditions with water cooling system. The circular surfaces were treated by acids and polished by a special polishing machine. The surface roughness of the specimens fell into the interval of 0.0001…0.0005 mm.

4. Results of the X-Ray Examination

The X-ray examinations were carried out at the ESRF synchrotron in Grenoble, at the ID22 Beamline. The beam has been monochromatized by a channel-cut silicon double crystal monochromator with no further optical element in the beam [2], [3]. This arrangement enabled long coherence length of the X-ray beam and phase contrast imaging of the voids produced by fatigue tests of the specimen. The beam size and the footprint on the specimen has been determined by a diaphragm of 0.5×0.5 mm in front of the specimen. The phase contrast images have been recorded by a special, high resolution two dimensional X-ray detector. A fluorescent crystal of about 0.5×0.5 mm aperture produced light signals which have been magnified by about $100\times$ by an optical microscope. This image has been recorded by a CCD plate in 1024 × 1024 pixels. The spatial resolution of this arrangement reached about 1 μm, linear resolution. The specimen was moved in the x-y directions perpendicular to the beam direction by several mm-s, however, no rotation has been performed. This means that the depth districbution of the voids has not been resolved in this measurements. The images seen in the different frames show a projection of the voids. The photos taken were directly scanned and stored on a compact disc. The single X-ray photos indicating the defects under a 0.5 mm × 0.5 mm real surface area of the thin disc-form specimen of 0.1 mm width were magnified resulting a 153 mm × 153 mm quadratic figure for the further image processing. In *Figs. 2* and *3* two photos are shown about the 'virgin' material and the loaded one undergone to fatigue test. The small disc-form specimen of the latter was processed from the close neighbourhood of the cross section of fatigue caused fracture of the specimen formerly used for fatigue tests.

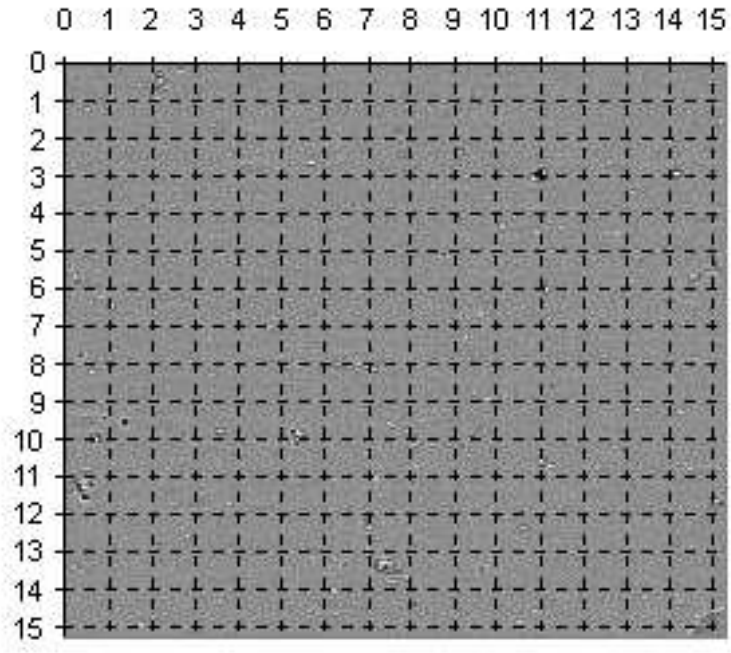

Fig. 2. X-ray photo of the virgin material, dimensions: 0.5 mm × 0.5 mm (photo No. 27)

5. Statistical Evaluation of the Figures

5.1. Introductory Remarks

The statistical evaluation of the X-ray photos was made in two main steps. The first step was the quantitative characterization of the defect-density both in virgin and damaged state of the material examined. The second step was the statistical analysis of the distribution of the defect dimensions. The latters were evaluated from the measured 'set-diameters' of the individual defects identified on the photos.

5.2. Probability Distribution of the Number of Defects in a Unit Volume

The data processing concerning the 'defect density' was based on the X-ray photos of 153 mm × 153 mm. As an initial step of the evaluation, an equidistant partition system of 10 mm step-length was taken along both axes, in order to define an orthogonal a 15 × 15 grid system. With the grid system defined set of small rectangles, the number of defects falling into a grid rectangle was determined.

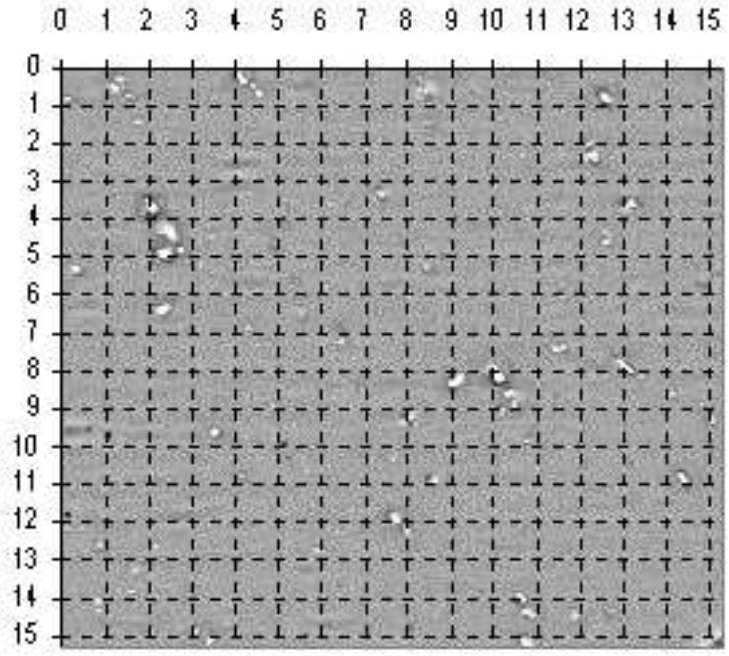

Fig. 3. X-ray photo of the damaged material, dimensions: 0.5 mm × 0.5 mm (photo No. 20)

For virgin material the number of defects found in the above specified small rectangles are indicated in *Table 1*. The total number of defects identified on the photo – in other words the sum of entries in *Table 1* - is 164. On the basis of the result received it is possible to estimate the mean defect density for the virgin material. Since the width of the specimen examined was $d = 0.1$ mm, and the real length belonging to 150 mm length on the photo is $x = 0.5(150/153) = 0.49019$ mm. Thus, the volume of the examined material is $V = x^2\, d = 0.0240286$ mm^3, and the mean value of the defect density can be identified: $\lambda = 6825\text{l/mm}^3$.

For damaged material the number of defects found in the small rectangles are indicated in *Table 2*. The total number of defects identified on the photo – in other words the sum of entries in *Table 2* - is 332. On the basis of the result received it is possible to estimate the mean defect density for the damaged material. Since the width of the specimen examined was $d = 0.1$ mm, and the real length belonging to 150 mm length on the photo is $x = 0.5(150/153) = 0.49019$ mm. Thus, the volume of the examined material is $V = x^2\, d = 0.0240286$ mm^3, and the mean value of the defect density can be identified: $\lambda = 13817\ \text{l/mm}^3$.

The second step of the evaluation was the determination of the relative fre-

Table 1. Matrix of measured defect frequencies in the volume partition elements of 0.0001085 mm^3 for virgin material. The total number of defects in the matrix is 164

0	1	5	0	0	0	0	0	0	1	0	0	0	0	0
1	0	0	1	0	1	0	2	0	0	0	2	0	0	1
0	0	0	0	1	3	1	1	1	1	2	2	1	0	1
1	0	0	2	0	0	0	0	0	2	1	1	0	1	0
0	0	0	1	2	1	0	0	0	1	2	3	1	2	5
3	0	0	2	1	1	0	0	1	0	0	0	0	0	0
2	1	0	1	0	0	0	0	0	2	0	1	0	1	0
1	0	0	0	1	0	0	1	0	2	0	0	1	0	4
1	0	0	1	0	0	3	1	0	2	1	0	0	0	0
3	1	0	1	0	3	0	2	3	1	0	0	0	1	1
1	0	0	0	0	2	1	1	4	3	0	3	1	0	1
5	0	1	1	1	1	2	0	0	0	0	0	0	1	2
0	0	1	0	0	0	3	0	0	0	1	0	1	0	2
3	0	0	0	0	1	0	5	0	1	1	0	0	0	0
0	1	0	2	0	1	1	1	0	0	2	0	0	0	2

quency distributions of the number of defects given by the entries in the rectangles of the matrices introduced. Both for the virgin and for the damaged materials the relative frequency histograms are shown in *Fig. 4*. As it can be observed, the shape of the histogram belonging to the virgin material more or less follows the expected 'Poisson rhythm', while the histogram belonging to the damaged material visibly deviates from the 'rhythm' mentioned, since the medium part of the diagram shows certain stagnation character.

5.3. Probability Distribution Function of the Defect Radii

The further evaluation goal concerning the X-ray photos was the characterization of the dimensions of the defects indicated. The 'set diameters' diam D of the visible defect domains D on the photos were defined by relation

$$\operatorname{diam} D = \max_{x,y \in D} \sqrt{(x_1 - x_2)^2 + (y_1 - y_2)^2}.$$

The diameters mentioned were determined by measuring the characteristic distances in *mm* on the 153 mm × 153 mm Figures shown in *Figs. 2* and *3*. The numerical values of the measured distances are introduced in *Tables 3* and *4* for the virgin and the damaged materials, respectively.

Table 2. Matrix of measured defect frequencies in the volume partition elements of 0.0001085 mm^3 for virgin material. The total number of defects in the matrix is 332.

0	5	0	0	4	2	0	0	4	0	0	0	1	0	3
1	2	1	1	0	1	3	3	3	2	0	1	1	1	2
0	0	0	0	0	0	2	1	0	2	4	2	1	1	0
0	0	3	0	1	1	1	2	0	3	5	0	5	1	0
0	0	3	1	5	4	1	0	1	0	1	2	2	0	0
5	0	2	7	3	3	1	0	4	0	0	1	1	1	4
1	0	4	2	4	2	0	0	0	0	0	2	0	1	1
1	0	1	1	3	0	3	0	0	2	1	5	4	0	0
0	0	0	0	3	4	4	2	2	4	4	0	2	3	3
1	4	0	1	0	3	0	2	2	1	5	0	0	0	2
0	4	2	0	3	4	0	1	1	3	2	0	1	1	0
3	0	0	0	0	0	3	3	0	1	1	1	1	2	0
0	3	3	3	1	3	1	4	5	0	0	3	0	0	1
2	8	3	2	0	0	2	0	0	2	2	1	2	1	0
1	0	2	4	1	4	2	0	0	0	3	4	3	0	0

Table 3:

virgin material	
row, column	micro crack diameters in mm
1.2	0.00197
1.3	0.00328 0.00361 0.00197 0.00164 0.00131
1.10	0.00098
2.1	0.00295
2.4	0.00492
2.6	0.00557
2.8	0.00311 0.00197
2.12	0.00180 0.00164
2.15	0.00328
3.5	0.00082
3. 6	0.00262 0.00033 0.00016
3.7	0.00246
3.8	0.00302
3.9	0.00033
3.10	0.00361
3.11	0.00066 0.00131
3.12	0.00164 0.00574

Table 3: (continued)

virgin material	
row, column	micro crack diameters in mm
3.13	0.00197
3.15	0.00459
4.1	0.00016
4.4	0.00131 0.00230
4.10	0.00279 0.00098
4.11	0.00525
4.12	0.00298
5.4	0.00262
5.5	0.00016 0.00033
5. 6	0.00039
5.10	0.00328
5.11	0.00295 0.00033
5.12	0.00197 0.00180 0.00049
5.13	0.00197
5.14	0.00200 0.00193
5.15	0.00164 0.00167 0.00167 0.00170 0.00066
6.1	0.00230 0.00197 0.00393
6.4	0.00262 0.00197
6.5	0.00197
6.6	0.00131
6.9	0.00262
7.1	0.00164 0.00036
7.2	0.00262
7.4	0.00082
7.10	0.00298 0.00213
7.12	0.00426
7.14	0.00344
8.1	0.00311
8.5	0.00279
8.8	0.00262
8.10	0.00131 0.00262
8.13	0.00279
8.15	0.00033 0.00098 0.00197 0.00197
9.1	0.00262
9.4	0.00295
9.7	0.00361 0.00328 0.00197
9.8	0.00393
9.10	0.00213 0.00207
9.11	0.00098
10.1	0.00262 0.00311 0.00492

Table 3: (continued)

virgin material	
row, column	micro crack diameters in mm
10.2	0.00426
10.4	0.00344
10.6	0.00393 0.00590 0.00033
10.8	0.00656 0.01639
10.9	0.00033 0.00066 0.00098
10.10	0.00262
10.14	0.00361
10.15	0.00393
11. 1	0.00311
11.6	0.00279 0.00344
11.7	0.00230
11.8	0.00197
11.9	0.00164 0.00164 0.00262 0.00279
11.10	0.00098 0.00262 0.00279
11.12	0.00361 0.00328 0.00230
11.13	0.00033
11.15	0.00066
12. 1	0.00262 0.00361 0.00393 0.00689 0.00590
12.3	0.00230
12.4	0.00246
12.5	0.00033
12.6	0.00131
12.7	0.00230 0.00213
12.14	0.00197
12.15	0.00033 0.00361
13.3	0.00098
13.7	0.00033 0.00131 0.00148
13.11	0.00279
13.13	0.00066
13.15	0.00115 0.00131
14.1	0.00066 0.00082 0.00098
14.6	0.00033
14.8	0.00984 0.00361 0.01311 0.00820 0.01148
14.10	0.00262
14.11	0.00230
15.2	0.00361
15.4	0.00295 0.00298
15.6	0.00361
15.7	0.00311
15.8	0.00098

Table 3: (continued)

virgin material	
row, column	micro crack diameters in mm
15.11	0.00197 0.00393
15.15	0.00230 0.00213

Table 4:

damaged material	
row, column	micro crack diameters in mm
1.2	0.00328 0.00525 0.00590 0.00295 0.00197
1.5	0.00393 0.01115 0.00344 0.00393
1.6	0.00754 0.00262
1.9	0.00246 0.00361 0.00918 0.00459
1.13	0.00656
1.15	0.00164 0.00148 0.00180
2.1	0.00393
2.2	0.00262 0.00361
2.3	0.00131
2.4	0.00098
2.6	0.00082
2.7	0.00262 0.00131 0.00082
2.8	0.00262 0.00262 0.00033
2.9	0.00325 0.00098 0.00262
2.10	0.00213 0.00230
2.1	0.00164
2.12	0.00262
2.13	0.00492
2.14	0.00262
2.15	0.00525 0.00033
3.7	0.00246 0.00262
3.8	0.00131
3.10	0.00230 0.00279
3.11	0.00262 0.00131 0.00246 0.00066
3.12	0.00361 0.00393
3.13	0.00492
3.14	0.00033
4.3	0.00328 0.00197 0.00918
4.5	0.00230
4.6	0.00311
4.7	0.00262

Table 4: (continued)

damaged material	
row, column	micro crack diameters in mm
4.8	0.00361 0.00311
4.10	0.00246 0.00197 0.00197
4.11	0.00262 0.00279 0.00246 0.00230 0.00197
4.13	0.00328 0.00361 0.00295 0.00098 0.00098
4.14	0.00361
5.3	0.01344 0.01639 0.00525
5.4	0.00311
5.5	0.00295 0.00295 0.00262 0.00230 0.00033
5.6	0.00262 0.00066 0.00082 0.00033
5.7	0.00262
5.9	0.00131
5.11	0.00262
5.12	0.00361 0.00131
5.13	0.00689 0.00262
6.1	0.00361 0.00328 0.00197 0.00213 0.00098
6.3	0.00820 0.00049
6.4	0.00393 0.00361 0.00328 0.00033 0.00033 0.00197 0.00033
6.5	0.00197 0.00262 0.00033
6.6	0.00098 0.00115 0.00262
6.7	0.00262
6.9	0.00656 0.00426 0.00262 0.00262
6.12	0.00279
6.13	0.00164
6.14	0.00131
6.15	0.01180 0.01311 0.00328 0.00918
7.1	0.00033
7.3	0.00262 0.00557 0.00393 0.00131
7.4	0.00230 0.00033
7.5	0.00393 0.00033 0.00033 0.00033
7.6	0.00295 0.00279
7.12	0.00262 0.00033
7.14	0.00197
7.15	0.00197
8.1	0.00361
8.3	0.00131
8.4	0.00115
8.5	0.00918 0.00295 0.00262
8.7	0.00852 0.00164 0.00098
8.10	0.00393 0.00754
8.11	0.00262

Table 4: (continued)

damaged material	
row, column	micro crack diameters in mm
8.12	0.00459 0.00426 0.00033 0.00033 0.00033
8.13	0.00426 0.00393 0.00393 0.00066
9.5	0.00295 0.00131 0.00066
9.6	0.00311 0.00295 0.00033 0.00033
9.7	0.00328 0.00361 0.00295 0.00230
9.8	0.00311 0.00098
9.9	0.00754 0.00098
9.10	0.00689 0.00361 0.00262 0.00230
9.11	0.00098 0.01016 0.00689 0.00230
9.13	0.00279 0.00098
9.14	0.00328 0.00311 0.00033
9.15	0.00361 0.00066 0.00033
10.1	0.00262
10.2	0.00361 0.00295 0.00262 0.00197
10.4	0.00590
10.6	0.00393 0.00328 0.00344
10.8	0.00459 0.00426
10.9	0.00426 0.00066
10.10	0.00033
10.11	0.00197 0.00033 0.00033 0.00033 0.00066
10.15	0.00328 0.00361
11.2	0.00426 0.00262 0.00230 0.00230
11.3	0.00033 0.00164
11.5	0.00262 0.00066 0.00033
11.6	0.00164 0.00131 0.00131 0.00033
11.8	0.00393
11.9	0.00492
11.10	0.00066 0.00098 0.00033
11.11	0.00098 0.00066
11.13	0.00262
11.14	0.01246
12.1	0.00426 0.00295 0.00295
12.7	0.00656 0.00262 0.00295
12.8	0.00393 0.00492 0.01148
12.10	0.00295
12.11	0.00066
12.12	0.00197
12.13	0.00164
12.14	0.00197 0.00033
13.2	0.00361 0.00361 0.00197

Table 4: (continued)

damaged material	
row, column	micro crack diameters in mm
13.3	0.00328 0.00197 0.00164
13.4	0.00328 0.00262 0.00033
13.5	0.00295
13.6	0.00852 0.00262 0.00262
13.7	0.00066
13.8	0.00361 0.00033 0.00033 0.00033
13.9	0.00197 0.00033 0.00033 0.00033 0.00033
13.12	0.00197 0.00131 0.00197
13.15	0.00656
14.1	0.00590 0.00066
14.2	0.00426 0.00361 0.00361 0.00328 0.00328 0.00197 0.00197 0.00098
14.3	0.00197 0.00033 0.00033
14.4	0.00131 0.00033
14.7	0.00230 0.00213
14.10	0.00098 0.00197
14.11	0.00393 0.00361
14.12	0.00262
14.13	0.00131 0.00131
14.14	0.00098
15.1	0.00098
15.3	0.00131 0.00066
15.4	0.00689 0.00623 0.00262 0.00033
15.5	0.00066
15.6	0.00164 0.00230 0.00230 0.00033
15.7	0.00197 0.00033
15.11	0.00459 0.00492 0.00393
15.12	0.00262 0.00262 0.00098 0.00197
15.13	0.00328 0.00131 0.00131

For crack propagation simulation purposes it is more convenient to use the crack radii instead of the directly measured diameters. In *Fig. 5* the empirical distribution functions of the crack radii are shown for the virgin, as well as for the damaged material.

It is interesting to recognize, that the two empirical distribution functions do not show great deviations, though, in accordance with the expectations, the distribution function of the damaged material is slightly dilated to the right in the region crack radii of dimension 0.0015…0.005 mm.

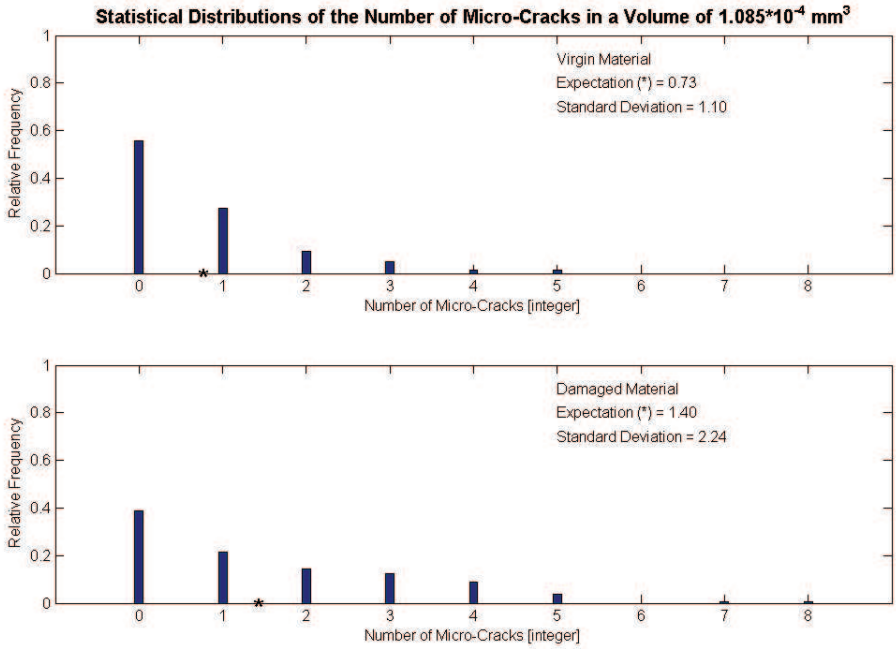

Fig. 4. Relative frequency histograms of the number of defects evaluated from the entries in the rectangles of the frequency matrices introduced for both materials in *Tables 1* and *2*

6. Conclusions

On the basis of the experimental results and the statistical evaluation procedures applied, the following conclusions can be drawn:

- The spatial distribution of defects estimated on the basis of a rectangular in space partition system of volume elements 0.0001085 mm^3 showed an approximate *Poisson rhythm* for the alloy-free steel examined in virgin state. The average defect density found for virgin material specimen was cca. 6800/mm^3. In case of damaged material specimen processed out from the close neighbourhood of the fractured cross section, the approximate *Poisson rhythm* disappear, and the mean damage density was cca. 13800/mm^3. This result means that the fatigue process leads to an *approximate doubling* in the number of defects recognizable in the framework of the applied X-ray technique and the subsequent statistical evaluation procedure.
- The defect dimensions were identified in the framework of a simple circular crack model. Surprisingly, the distributions of crack radii for the virgin and damaged material specimens showed only very small deviations. For

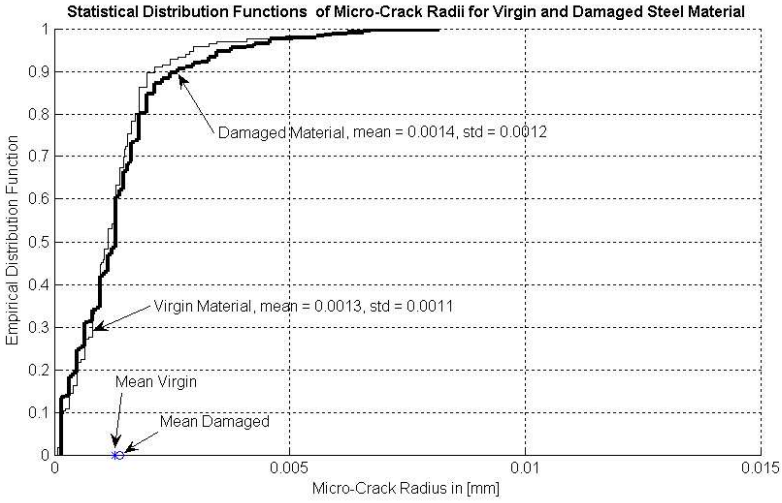

Fig. 5. Empirical distribution functions of micro crack radii for virgin and damaged steel material

example the mean crack radius for the virgin material was 0.0013 mm, while for the damaged material the mean radius obtained was 0.0014 mm. The related dispersions were also in the close neighbourhood of each other, namely values 0.0011 mm and 0.0012 mm were experienced. All these leads to the conjecture that the load repetition in the bulk material (where no rapid crack propagation causing final fracture occurs) causes an increase in the number of recognizable cracks, but the dimensions of the initially existing cracks grow very slowly. The rapid crack, causing the final fracture of the test specimen is probably started from a 'dominating' initial micro crack having an initial radius in the close neighbourhood of the possible maximum crack radius values.

- Further research is necessary for the elaboration of more exact identification procedures for analysing the crack geometries – both the shape and orientation conditions. The application of the new methods of automated image processing technique is also a crucial tool of the future research.

7. Acknowledgement

Authors express their cordial thanks to Prof. László Dévényi and Prof. Péter János Szabó, staff members of the Department of Material Science and Mechanical Technology at the BME for their help in energy dispersion X-ray analysis for determining the mass-spectrogram of the steel material examined. Furthermore the authors are greatly indebted

for the Hungarian Scientific Research Fund OTKA for supporting the present research project.

References

[1] HALÁSZ, G. – MÁRIALIGETI, J. – ZOBORY, I., Statistical Methods in the Engineering Practice. An Issue of the Institute for Postgraduate Studies in Engineering of the BME (5028). Budapest, 1976. (In Hungarian).

[2] KOHN, V. – SNIGIREVA, I. – SNIGIREV, A., Interferometric Characterization of Spatial Coherence of High Energy Synchrotron X-rays, *Optics Communications,* **198** (2001), pp. 293–309.

[3] SNIGIREV, A. – SNIGIREVA, I. – KOHN, V. G. – KUZNETSOV, S. M., On the Requirements to the Instrumentation for the New Generation of the Synchrotron Radiation Sources, Beryllium Windows, *Nuclear Instruments and Methods in Physics Research*, **A 370** (1996), pp. 634–640.